PHYSICAL REVIEW B **82**, 041202(R) (2010)

Magnetism of Co doped ZnO with Al codoping: Carrier-induced mechanisms versus extrinsic origins

A. Ney,* V. Ney, S. Ye, K. Ollefs, and T. Kammermeier
Fakultät für Physik and CeNIDE, Universität Duisburg-Essen, Lotharstr. 1, D-47057 Duisburg, Germany

T. C. Kaspar and S. A. Chambers
Fundamental and Computational Sciences Directorate, Pacific Northwest National Laboratory, Richland, Washington 99352, USA

F. Wilhelm and A. Rogalev
European Synchrotron Radiation Facility (ESRF), 6 Rue Jules Horowitz, BP 220, 38043 Grenoble Cedex, France
(Received 18 May 2010; revised manuscript received 9 July 2010; published 23 July 2010)

$Zn_{1-x}Co_xO$ epitaxial films codoped with Al were studied using a combination of synchrotron-based x-ray absorption spectroscopies and classical magnetometry. Phase purity was verified by comparing the x-ray linear dichroism with simulations and previously published reference spectra. The existence of weak ferromagnetism or inhomogeneous superparamagnetism is evidenced at low temperatures by classical magnetometry. A combination of x-ray absorption spectroscopies indicates that its origin is most likely of extrinsic character such as magnetic impurities or the onset of phase separation rather than weak, electron mediated ferromagnetism.

DOI: 10.1103/PhysRevB.82.041202 PACS number(s): 75.50.Pp, 71.55.Gs, 75.70.−i

Dilute magnetic semiconductors (DMS) which exhibit ferromagnetism (FM) at and above room temperature are a highly desirable class of materials for future spintronics devices. $Zn_{1-x}Co_xO$ (Co:ZnO) is a heavily studied DMS material in this context. Although controversially discussed in the literature, there is a growing consensus, that phase-pure Co:ZnO is paramagnetic (PM).[1–3] Altering the preparation conditions can easily lead to phase separation and consequently superparamagnetism (SPM).[3] Nonetheless there are recent experimental data claiming that FM can be switched on in Co:ZnO by controlling the carrier concentration.[4] On the other hand, no FM was found in structurally excellent Al-codoped Co:ZnO.[5] However, in the latter work the magnetic characterization was restricted to room-temperature measurements. In parallel, theory has also revealed that defect-free, insulating Co:ZnO is not ferromagnetic[6,7] whereas the role of *n*-type carriers remains under debate, ranging from ferromagnetic coupling,[8] or oscillatory behavior with Co-Co distance[9] to antiferromagnetic coupling.[10] It is rather common to manipulate the *n*-type carrier concentration of ZnO by Al doping to yield high conductivity.[4,11] On the other hand, it had been shown that Al codoping of Co:ZnO may promote the onset of phase separation.[11] It is extremely difficult to detect such secondary Co-containing phases even with the most careful x-ray diffraction (XRD) analysis[11,12] or depth-profiling photoelectron spectroscopy (DP-XPS).[13] This type of materials characterization is lacking in Ref. 4. A highly sensitive alternative to XRD or DP-XPS to look for potential phase separation in Co:ZnO is the combination of x-ray absorption near-edge spectra (XANES), x-ray linear dichroism (XLD), and x-ray magnetic circular dichroism (XMCD). This suite of atom-specific x-ray spectroscopies nicely complements integral superconducting quantum interference device (SQUID) magnetometry. For example, combined XLD simulations and experiments at the Co *K* edge have been used to verify the phase purity of Co:ZnO (Ref. 2) and characteristic spectroscopic signatures with appropriate quality thresholds for PM and SPM have been identified recently in the XANES and XMCD at the Co *K* edge of Co:ZnO.[3] Along the same line, a careful combination of XANES and extended x-ray absorption fine structure (EXAFS) was employed to study Co:ZnO films similar to those in Ref. 4 which found evidence for Co(0) secondary phases.[14]

Here we use the approach of combined SQUID magnetometry and element specific XANES, XLD, and XMCD to study Al-codoped Co:ZnO epitaxial films with low resistivity. Weak FM-like signatures are found by SQUID but only at low temperatures. However, this behavior cannot be connected to electron-mediated ferromagnetism of Co by dopant-specific spectroscopies. It merely originates from either traces of magnetic impurities or the onset of phase separation. These results imply that previous observations of ferromagnetism in *n*-type Co:ZnO such as those reported in Ref. 4 are instead due to secondary phase formation as indicated by XANES and EXAFS measurements.[14] Without quantitative insight from these dopant-specific spectroscopies, claims of carrier-mediated ferromagnetism raise false hopes about Co:ZnO as a true, carrier-mediated *n*-type DMS.

Al-codoped Co:ZnO(0001) epitaxial films with a thickness around 100 nm were grown on epiready *c*-plane sapphire substrates by pulsed laser deposition as described elsewhere.[5] A number of samples were screened by SQUID with the magnetic field applied in the film plane and all measurement artifacts as described in Ref. 19 corrected; signals below 0.4 μemu were disregarded. Before measuring $M(T)$ while warming at 10 mT, the sample was either field cooled (FC) from 300 K to 5 K in 4 T or zero-field cooled (ZFC) after demagnetizing in an oscillatory field at 300 K. The diamagnetic background has been derived from the $M(H)$ behavior at high fields at 300 K and was subtracted from all data. In stark contrast to the findings in Ref. 4, none of the samples exhibits strong FM-like signatures at room

temperature, consistent with Ref. 5. Only at low temperatures were weak signs of FM-like behavior [separation of FC and ZFC $M(T)$ curves] found. No clear SPM behavior (clear maximum in the ZFC curve) was visible. We illustrate using measurements from a 65-nm-thick 6 at. % Co:ZnO film (as measured with a combination of proton-induced x-ray emission (PIXE) and Rutherford backscattering spectroscopy) with nominally 1 at. % of Al codoping (Al:Co:ZnO) which exhibited the most pronounced FM-like signatures. The resistivity ρ of this strongly n-type film was determined to be 0.001 Ω cm at room temperature, i.e., metallic according to the criteria in Ref. 4. For this specimen hard x-ray absorption spectra were taken at the ESRF ID 12 beamline in total fluorescence yield[15] offering sensitivity over a micron depth scale. Note that in the soft x-ray regime it is particularly difficult to sense the interface to the substrate since total electron yield measurements probe only the first few nanometers of the film[16] and for the fluorescence yield a probing depth of approx. 100 nm can be achieved.[17] Even for a 65 nm film this depth sensitivity may not be sufficient to probe the contribution of atoms located at the interface, especially directly at the maximum absorption, where the probing depth is in general smaller due to increased self-absorption. The XLD and XMCD measurements were carried out at 10° and 15° grazing incidence, respectively, under identical conditions as in Ref. 2. The XLD and XANES spectra were simulated with the FDMNES code[18] using a multiple scattering formalism within the muffin tin approximation.

Figure 1 shows the integral magnetic characterization by SQUID for the Al:Co:ZnO sample. It is clear from Fig. 1(a) that the specimen is predominantly PM with a tiny (corresponding to at most 1% of the Co being ferromagnetic) magnetic component at 300 K. This signal is of the order of 1 μemu and is thus only slightly above the estimated detection limit of the SQUID magnetometer (0.2–0.4 μemu) for this type of specimen.[19] At 5 K the sample exhibits hysteretic $M(H)$ behavior at low magnetic fields as shown in Fig. 1(b). The corresponding quality indicator according to Ref. 3 is larger than 60, i.e., just in the middle of the PM-SPM range. Figure 1(c) reveals that the Al:Co:ZnO sample shows little if any maximum in the ZFC curve although a clear separation between FC and ZFC is visible below ~100 K, in agreement with the presence of a magnetic hysteresis at 5 K. Therefore, SQUID points to either a weak and very inhomogeneous SPM (very broad size and/or anisotropy distribution of the phase-separated nanoclusters) or weak FM-like behavior at low temperatures. Note that, in principle, such magnetic behavior can also originate from magnetic contamination of the substrate[19,20] and great care was taken minimize this effect for this series of samples by etching the substrates prior to the deposition of the film and checking cleanliness by room-temperature magnetometry as described in Ref. 5.

Figure 2 summarizes the x-ray absorption results for the Al:Co:ZnO sample in comparison to a representative PM phase-pure Co:ZnO reference specimen (blue dashed-dotted line).[2,3] The XANES in Fig. 2(a) for both samples are virtually identical, indicating that the Co is predominantly present in a formal 2+ oxidation state in tetrahedral coordination. The enlargement of the pre-edge feature shown in the inset of Fig. 2(a) reveals no significant differences between the

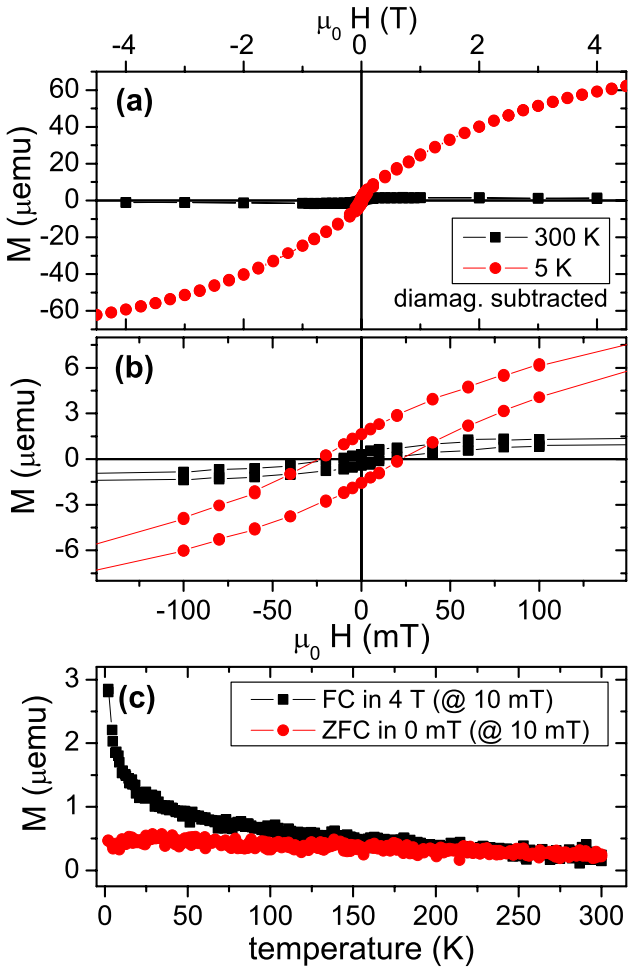

FIG. 1. (Color online) SQUID $M(H)$ curves for a Al-codoped Co:ZnO film. (a) $M(H)$ curves measured at 300 K and 5 K, respectively, and (b) enlargement of the low-field region. (c) $M(T)$ behavior recorded after field-cooled and zero-field-cooled conditions. The diamagnetic background has been subtracted from all data sets.

PM Co:ZnO and the Al:Co:ZnO samples, and the latter reaches a XANES quality indicator of 1.76, which is in the middle of the quality threshold region in Ref. 3. This indicates that Co in the Al:Co:ZnO sample does not exhibit any measurable elemental character[3] although the conductivity is much larger than that of the PM sample. The corresponding XLD signatures of both specimens are displayed in Fig. 2(b). The magnitude of the XLD is a measure of the fraction of the Co dopant atoms incorporated on Zn lattice sites. The XLD signal of the Al:Co:ZnO sample is only reduced by at most 5% in comparison to the phase-pure PM reference, yielding a quality indicator of 0.59 which is just at the lower limit of the quality threshold region in Ref. 3. This result may indicate the very onset of phase separation. On the other hand, if the XLD signatures are simulated using the identical parameters as in Ref. 2 the XLD signature is slightly decreased when an Al atom is placed on one of the 12 next-cation-neighbor sites around the Co atom (red triangles). Therefore, in the case of the Al:Co:ZnO sample, the reduction of the XLD may also be caused by the Al codopant atoms. Al codoping, which increases the carrier concentration consid-

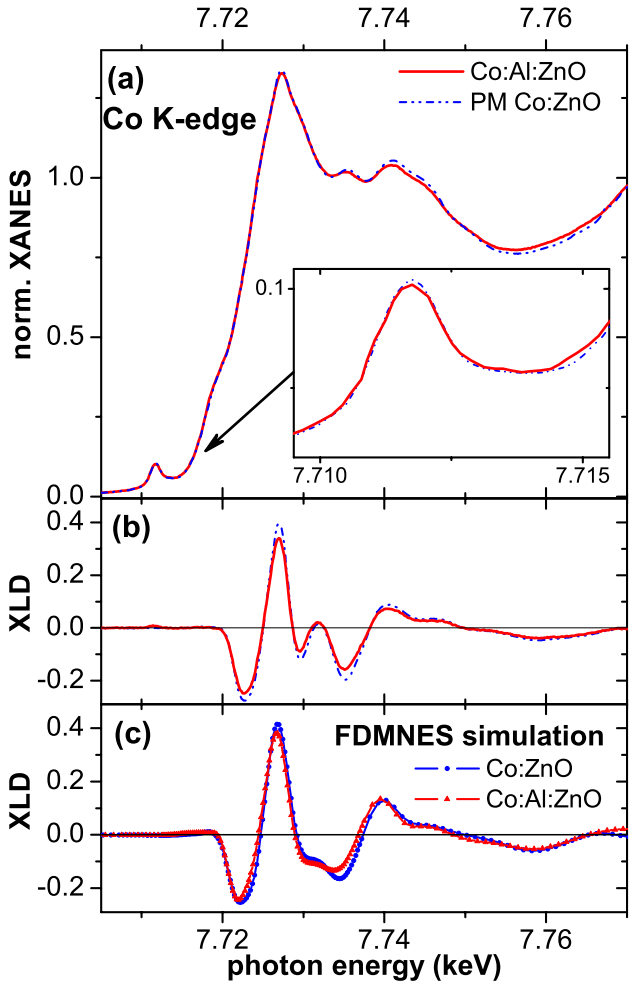

FIG. 2. (Color online) (a) XANES spectra at the Co K edge for a representative Al:Co:ZnO film and a typical PM Co:ZnO sample; the pre-edge region is enlarged in the inset. (b) XLD for the same two films. (c) Simulations of the XLD for pure Co:ZnO and Co:ZnO with Al on the cation site adjacent to the Co.

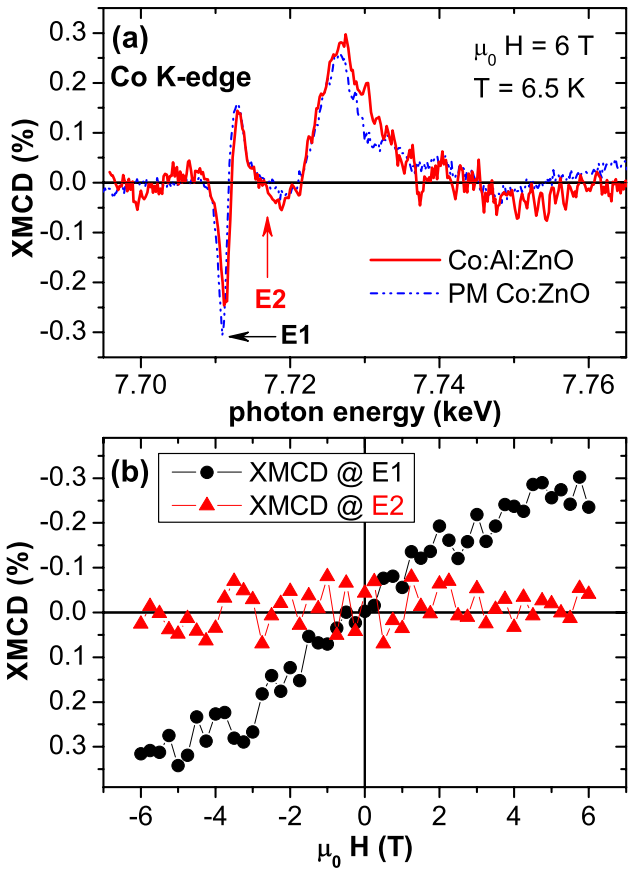

FIG. 3. (Color online) (a) XMCD spectra for the Al:Co:ZnO sample in comparison to the reference specimen recorded at 6 K and 6 T. Two characteristic energies E_1 and E_2 are marked at which the element specific $M(H)$ curves in (b) were measured.

erably, has a reducing effect on the XLD, presumably due to slight screening of the crystal field of the surrounding O anions. Because these carriers do not promote a more elemental character of the Co as evidenced by the pronounced pre-edge feature shown in Fig. 2(a), it can be concluded, that the Co incorporation on Zn lattice sites in Al:Co:ZnO is nearly the same as in the reference PM Co:ZnO specimen.

Figure 3 shows the XMCD, which is element specific magnetometry for the Al:Co:ZnO sample compared to that for the PM reference specimen. The spectra shown in Fig. 3(a) were recorded at 6.5 K at 6 T with the magnetic field oriented in the film plane ($H \perp c$). As already discussed in Ref. 3, there are two characteristic spectral features which can help elucidate the origin of the magnetic behavior. One is the magnitude of the pre-edge feature which reflects the magnetic response of Co^{2+} in tetrahedral coordination and is best measured at photon energy E_1. The Al:Co:ZnO specimen shows a quality indicator of 0.39% which is in the PM regime[3] although it is slightly reduced compared to the PM reference in Fig. 3(a). The second magnetic contribution is best measured at E_2 where only elemental or metallic Co exhibit nonzero XMCD. The Al:Co:ZnO specimen yields an XMCD intensity of less than 0.03% which is clearly within the PM regime.[3] At both energies an element specific $M(H)$ curve has been measured for the Al:Co:ZnO sample and the results are shown in Fig. 3(b). A paramagnetic response is observed at E_1, as expected, and this accounts for the prevailing paramagnetic $M(H)$ behavior which has already been seen by SQUID, see Fig. 1(a). The small magnetic component, which gives rise to the FC/ZFC separation and the hysteresis at 5 K in SQUID measurements, cannot be resolved in the K-edge XMCD at E_1 since the signal-to-noise ratio at low magnetic fields is not sufficient to detect the hysteresis. In contrast, at E_2, where Co metal exhibits the maximum XMCD signal, a finite magnetic contribution would quickly saturate with magnetic field and should be visible as a step-like behavior in the XMCD(H) data in the measured field range, i.e., between ± 1 T and ± 6 T. However, no signal exceeding the noise of the measurement is visible. This finding is in agreement with a negligible XMCD signal at E_2 which is of the same size as for the PM reference specimen, see Fig. 3(a). Thus, no significant magnetic contribution stemming from Co with elemental/metallic character was found.

These XANES/XLD results show that making structurally excellent Co:ZnO highly n type by the addition of an elec-

tronic dopant such as Al does not degrade the structural quality or drive reduction in substitutional Co^{2+}, leading to magnetic secondary phase formation. The Co-specific dichroism in Fig. 3 within the accuracy of the measurement shows a purely paramagentic response at the photon energy appropriate for Co^{2+} in tetrahedral coordination (E_1) and no measurable response at the energy sensitive to Co(0) (E_2). The slight hysteresis seen at 5 K in the SQUID loop (Fig. 1) may thus be due to trace quantities of magnetic impurities which go undetected in room temperature magnetometry employed to check the magnetic cleanliness of the etched substrates. Alternatively, tiny amounts of Co-O secondary phases—as found in Co:ZnO films prepared by reactive magnetron sputtering—can account for the low-temperature magnetic response in SQUID measurements.[3] Note that the magnetic hysteresis and the FC/ZFC separation of the Co:Al:ZnO film studied here is much smaller than for any of the superparamagnetic samples studied in Ref. 3. Therefore, the magnetic response seen by volume averaged SQUID magnetometry can only be attributed to a tiny fraction—if any—of the Co dopant atoms and an intrinsic origin of the magnetic properties is highly unlikely. The existence of electron-mediated ferromagnetism at room temperature among the substitutional Co^{2+} dopants cannot be confirmed neither by SQUID nor by the XMCD loop at E_1 in Fig. 3 which is predominantly paramagnetic. Note, that the role of defects for the magnetic order cannot directly be studied using these techniques since they do not exhibit characteristic spectroscopic signatures.

In summary, we show that when care is taken to ensure that structural quality is maintained, thermally robust ferromagnetism does not result from electronic doping of Co:ZnO with Al. These results contradict those of Ref. 4 and secondary phases such as Co(0) as found in Ref. 14 for similar samples provide evidence that the observed ferromagnetism does not stem from an intrinsic carrier-mediated mechanism. Nonetheless, the influence of defects on the magnetic properties as recently highlighted in Ref. 21 remains open. On the other hand, defects were not explicitly discussed in Ref. 4 and also go beyond the scope of the present paper which focuses on the role of the carriers. This work demonstrates the need for dopant-specific x-ray absorption and linear dichroism to establish charge state and local structure, respectively, along with magnetic circular dichroism at the dopant absorption edge to determine the magnetic properties of the dopant. Only when these data are obtained can volume averaged magnetometry measurements be defensibly connected to the intrinsic magnetic properties of dilute magnetic oxides.

A.N. gratefully acknowledges financial support from the German Research Foundation (DFG) within the Heisenberg-Programm. The early stage of this work was in parts supported by the European Union under the Marie-Curie Excellence Grant No. MEXT-CT-2004-014195 of the sixth Framework Programme. A portion of the research was performed using EMSL, a national scientific user facility sponsored by the Department of Energy's Office of Biological and Environmental Research located at Pacific Northwest National Laboratory.

*andreas.ney@uni-due.de

[1] P. Sati, C. Deparis, C. Morhain, S. Schäfer, and A. Stepanov, Phys. Rev. Lett. **98**, 137204 (2007).

[2] A. Ney, K. Ollefs, S. Ye, T. Kammermeier, V. Ney, T. C. Kaspar, S. A. Chambers, F. Wilhelm, and A. Rogalev, Phys. Rev. Lett. **100**, 157201 (2008).

[3] A. Ney, M. Opel, T. C. Kaspar, V. Ney, S. Ye, K. Ollefs, T. Kammermeier, S. Bauer, K.-W. Nielsen, S. T. B. Goennenwein, M. H. Engelhard, S. Zhou, K. Potzger, J. Simon, W. Mader, S. M. Heald, J. C. Cezar, F. Wilhelm, A. Rogalev, R. Gross, and S. A. Chambers, New J. Phys. **12**, 013020 (2010).

[4] A. J. Behan, A. Mokhtari, H. J. Blythe, D. Score, X.-H. Xu, J. R. Neal, A. M. Fox, and G. A. Gehring, Phys. Rev. Lett. **100**, 047206 (2008).

[5] T. C. Kaspar, T. Droubay, S. M. Heald, P. Nachimuthu, C. M. Wang, V. Shutthanandan, C. A. Johnson, D. R. Gamelin, and S. A. Chambers, New J. Phys. **10**, 055010 (2008).

[6] C. H. Patterson, Phys. Rev. B **74**, 144432 (2006).

[7] S. J. Hu, S. S. Yan, M. W. Zhao, and L. M. Mei, Phys. Rev. B **73**, 245205 (2006).

[8] E. C. Lee and K. J. Chang, Phys. Rev. B **69**, 085205 (2004).

[9] S. K. Nayak, M. Ogura, A. Hucht, H. Akai, and P. Entel, J. Phys.: Condens. Matter **21**, 064238 (2009).

[10] D. Iuşan, R. Knut, B. Sanyal, O. Karis, O. Eriksson, V. A. Coleman, G. Westin, J. M. Wikberg, and P. Svedlindh, Phys. Rev. B **78**, 085319 (2008).

[11] M. Venkatesan, P. Stamenov, L. S. Dorneles, R. D. Gunning, B. Bernoux, and J. M. D. Coey, Appl. Phys. Lett. **90**, 242508 (2007).

[12] M. Opel, K.-W. Nielsen, S. Bauer, S. T. B. Goennenwein, J. C. Cezar, D. Schmeisser, J. Simon, W. Mader, and R. Gross, Eur. Phys. J. B **63**, 437 (2008).

[13] T. C. Kaspar, T. Droubay, S. M. Heald, M. H. Engelhard, P. Nachimuthu, and S. A. Chambers, Phys. Rev. B **77**, 201303(R) (2008).

[14] S. M. Heald, T. C. Kaspar, T. Droubay, V. Shutthanandan, S. A. Chambers, A. Mokhtari, A. J. Behan, H. J. Blythe, J. R. Neal, A. M. Fox, and G. A. Gehring, Phys. Rev. B **79**, 075202 (2009).

[15] A. Rogalev, J. Goulon, C. Goulon-Ginet, and C. Malgrange, Lect. Notes Phys. **565**, 61 (2001).

[16] S. J. Naftel and T. K. Sham, J. Synchrotron Radiat. **6**, 526 (1999).

[17] B. L. Henke, P. Lee, T. J. Tanaka, R. L. Shimabukuro, and B. K. Fujikawa, At. Data Nucl. Data Tables **27**, 1 (1982).

[18] Y. Joly, Phys. Rev. B **63**, 125120 (2001).

[19] A. Ney, T. Kammermeier, V. Ney, K. Ollefs, and S. Ye, J. Magn. Magn. Mater. **320**, 3341 (2008).

[20] R. Salzer, D. Spemann, P. Esquinazi, R. Höhne, A. Setzer, K. Schindler, H. Schmidt, and T. Butz, J. Magn. Magn. Mater. **317**, 53 (2007).

[21] J. M. D. Coey, J. T. Mlack, M. Venkatesan, and P. Stamenov, IEEE Trans. Magn. **46**, 2501 (2010).